Stability Analysis of Unsteady Ablation Fronts

The classical Rayleigh-Taylor instability[1] occurs when a heavy fluid is accelerated by a lighter fluid. In inertial-confinement fusion (ICF) the heavy fluid is the compressed ablated target material that is accelerated by the low-density ablated plasma. The classical treatment of the incompressible Rayleigh-Taylor instability leads to a linear growth rate given by $\gamma = \sqrt{|kg|A}$, where k is the instability wave number, g is the acceleration, and A is the Atwood number $A = (\rho_h - \rho_l)/(\rho_h + \rho_l)$. ($\rho_l$ and ρ_h represent the light- and heavy-fluid densities, respectively.) For typical (ICF) parameters, a classical Rayleigh-Taylor instability would produce an unacceptably large amount of distortion in the unablated target, resulting in a degraded capsule performance with respect to the final core conditions. Thus, it is important to study the possible means for suppression of the ablation surface instability in ICF. It has been recently shown that the ablation process leads to convection of the perturbation away from the interface between the two fluids.[2–5] Since the instability is localized at the interface, the ablative convection stabilizes short-wavelength modes. The typical growth rate of the ablative Rayleigh-Taylor instability can be written in the following approximate form:[3]

$$\gamma = \sqrt{|kg|A} - \beta|kV_a| , \tag{1}$$

where V_a is the ablation velocity and β is a numerical factor $(\beta \simeq 3-4)$.

In this article we show that a properly selected modulation of the laser intensity can significantly reduce the unstable spectrum and the maximum growth rate. To treat the analytic linear stability of unsteady ablation fronts, we consider a simplified sharp boundary model consisting of a heavy fluid, with density ρ_h, adjacent to a lighter fluid (ρ_l), in the force field $\mathbf{g}(t) = g(t)\mathbf{e}_y$ in a direction opposite to the density gradient [$g(t) < 0$ and $\mathbf{e}_y$ is the unit vector in the direction of the density gradient] and with an arbitrary time dependence. The heavy fluid is moving downward with velocity $\mathbf{U}_h = -V_a\mathbf{e}_y$, and the lighter fluid is ejected with velocity U_l. The equilibrium velocities $U_l(t)$ and $U_h(t)$ are both dependent on the ablation ratio per unit surface $\dot{m}(t)$ that is treated as an arbitrary function of time. The equilibrium can be readily derived from conservation of mass and momentum. We consider a class of equilibria with nonuniformities localized at the interface between the two fluids. Continuity of the mass flow and the pressure balance across the interface lead to the following conditions:

$$\rho_l U_l(t) = \rho_h U_h(t) \tag{2}$$

$$P_h - P_l = \rho_l U_l^2(t) - \rho_h U_h^2(t) , \tag{3}$$

where P_h and P_l represent the pressure of the heavy and light fluid, respectively, at the interface. Notice that U_l and U_h are negative in the chosen frame of reference. We assume that the discontinuities in the equilibrium quantities can be removed by including the physics of the ablation process.

The linear stability problem can be greatly simplified by an appropriate choice of the linearized equation of state. It is widely known that the most Rayleigh-Taylor unstable perturbations are incompressible. Furthermore, ablative stabilization is a convective process and is, therefore, independent of the equation of state. It follows that the essential physics of the instability can be captured by a simple incompressible flow model. The stability analysis proceeds in a standard manner. All perturbed quantities are written as $Q_1 = \tilde{Q}(y,t)\exp(ikx)$, and the system of equations describing the linear evolution of the perturbation assumes the following form:

$$\begin{aligned} &\left(\partial_t + U_j\partial_y\right)\tilde{\rho}_j = 0, \\ &\rho_j\left(\partial_t + U_j\partial_y\right)\tilde{v}_{jx} = -ik\tilde{p}_j \\ &\rho_j\left(\partial_t + U_j\partial_y\right)\tilde{v}_{jy} + \tilde{\rho}_j\partial_t U_j = -\partial_y\tilde{p}_j + \tilde{\rho}_j g \\ &ik\tilde{v}_{jx} + \partial_y\tilde{v}_{jy} = 0, \end{aligned} \tag{4}$$

where the subscript j denotes the heavy fluid region ($j = h$) and the light fluid region ($j = l$) and $\partial_y = \partial/\partial y$, $\partial_t = \partial/\partial t$. The two regions are separated by an interface (the ablation front) that moves with the heavy fluid. In order to match the solutions in the two regions, an equation describing the evolution of the interface is needed. Such an equation can be easily derived by a comparison with a nonablative equilibrium ($U_h = 0$). In that case the interface $\left[y = \tilde{\eta}(t)\exp(ikx)\right]$ moves with the heavy fluid, and the rate of distortion $\left(\partial_t\tilde{\eta}\right)$ is equal to the normal component of the velocity, $\partial_t\tilde{\eta} = \tilde{v}_{hy}(y = 0, t)$. In the ablative case, the heavy fluid is moving toward the ablation front with velocity $U_h = -V_a$. A Lagrangian surface, coming from $y = +\infty$, would become distorted as it approaches the interface where the instability is localized (Fig. 57.1). As for static equilibria, the rate of distortion $\left(\tilde{\xi}\right)$ of that surface is still equal to the normal component of the velocity:

$$\frac{d\tilde{\xi}}{dt} = \tilde{v}_{hy}. \tag{5a}$$

However, since the surface is moving, the time derivative has to be convective $\left(d_t = \partial_t + U_h\partial_y\right)$. From Eq. (5a) the distortion of a Lagrangian surface can be written in the following integral form:

$$\tilde{\xi}(t) = \int_{-\infty}^{t} \tilde{v}_{hy}\left[y_0(t'), t'\right]dt', \tag{5b}$$

where

$$y_0(t') = \int^{t'} U_h(t'')dt'' + constant$$

is the unperturbed trajectory of a Lagrangian surface. In the absence of smoothing effects, the ablation front coincides with that Lagrangian surface whose equilibrium orbit overlaps the ablation front ($y = 0$) at time $t' = t$. The unperturbed trajectory of such a surface is given by

$$y_0(t') = \int_t^{t'} U_h(t'')dt'',$$

and the equation for the evolution of the ablation front $\left(\tilde{\eta}\right)$ can be written in the following differential form:

$$\partial_t\tilde{\eta} = \tilde{v}_{hy}[0,t] - U_h(t)\int_{-\infty}^{t} \frac{\partial\tilde{v}_{hy}}{\partial y}\left[y_0(t'), t'\right]dt'. \tag{5c}$$

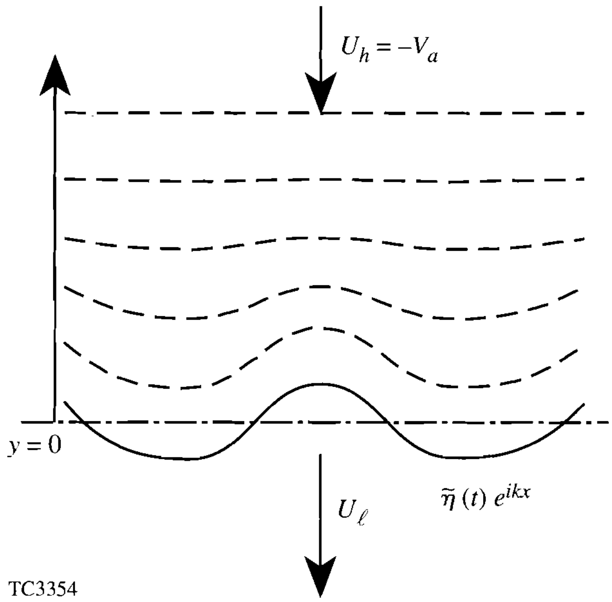

Figure 57.1
Deformation of a Lagrangian surface approaching the ablation front.

Once $\tilde{\eta}$ is known, a set of jump conditions relating the values of the physical quantities in the two regions can be derived by writing the time derivative of any perturbed quantity at the ablation front as $\partial_t\tilde{Q} = -\left(Q_h - Q_l\right)\partial_t\tilde{\eta}\,\delta(y)$ and integrating the incompressibility and conservation equations across the thin ablative layer. A short calculation yields

$$\begin{aligned}
&\tilde{v}_{hy} = \tilde{v}_{ly}\\
&\left(\rho_h - \rho_l\right)\left(\partial_t\tilde{\eta} - \tilde{v}_{hy}\right) - U_h\tilde{\rho}_h + U_l\tilde{\rho}_l = 0\\
&\tilde{v}_{hx} - \tilde{v}_{lx} + ik\tilde{\eta}\left(U_h - U_l\right) = 0\\
&\tilde{p}_h - \tilde{p}_l + \tilde{\rho}_h U_h^2 - \tilde{\rho}_l U_l^2 + g\left(\rho_h - \rho_l\right)\tilde{\eta} = 0.
\end{aligned} \tag{6}$$

The first of Eqs. (6) follows directly from the incompressibility condition $\nabla \cdot \tilde{\mathbf{v}} = 0$. A better representation of the perturbation at the interface can be obtained by using an equation of state and calculating the jump in the energy.[2] This approach would greatly complicate the calculation. However, as shown in Appendix A, when the flow is subsonic

$$\left[U_h^2, U_l^2 << p_h/\rho_h, p_l/\rho_l\right],$$

the flow of internal energy across the interface has to be conserved and the incompressible result is recovered.

The next step is to solve Eqs. (4) in the two regions and then apply the jump conditions and the boundary conditions at $y = \pm\infty$. Since the heavy and light fluids extend to infinity and the instability is localized at the interface, the perturbation must vanish at $y = \pm\infty$.

The solution of the linearized equation in the heavy-fluid region (h) is greatly simplified by the following transformation: $y_h = y - \int_0^t U_h(t')dt'$. A straightforward calculation leads to the following form of the perturbed variables in region h:

$$
\begin{aligned}
\tilde{v}_{hy} &= \tilde{u}_h(t)\exp(-ky_h) + \tilde{a}(y_h) \\
\tilde{v}_{hx} &= \frac{i}{k}\frac{\partial \tilde{v}_{hy}}{\partial y_h} \\
\tilde{\rho}_h &= \tilde{\rho}_h(y_h) \\
\tilde{p}_h &= -\frac{\rho_h}{k^2}\frac{\partial^2 \tilde{v}_{hy}}{\partial t \partial y_h} ,
\end{aligned}
\tag{7}
$$

where $\tilde{u}_h(t)$, $\tilde{\rho}_h(y_h)$, and $\tilde{a}(y_h)$ are arbitrary functions of t and y_h, and k is chosen to be positive $(k > 0)$. In order to satisfy the boundary conditions, $\tilde{a}$ and $\tilde{\rho}_h$ must vanish at $y_h \to \infty$. Since $\lim_{t\to\infty} y_h = \infty$, it follows that $\tilde{a}$ and $\tilde{\rho}_h$ asymptotically vanish in time. In our asymptotic stability analysis, we neglect all the quantities that do not grow in time. Thus, we set $\tilde{a} = 0$ and $\tilde{\rho}_h = 0$. Furthermore, because of the incompressibility condition and negative flow velocity, $\tilde{\rho}_h = 0$ at all times.

We apply the same procedure to the light-fluid region (l) and define the new coordinates $y_l = y - \int_0^t U_l(t')dt'$. The solution of the linearized equations in region l can be written in the following form:

$$
\begin{aligned}
\tilde{v}_{ly} &= \tilde{u}_l(t)\exp(ky_l) + \tilde{b}(y_l) + \tilde{c}(y_l)f(t) \\
\tilde{v}_{lx} &= \frac{i}{k}\frac{\partial \tilde{v}_{ly}}{\partial y_l} \\
\tilde{\rho}_l &= \tilde{\rho}_l(y_l) \\
\tilde{p}_l &= -\frac{\rho_l}{k^2}\frac{\partial^2 \tilde{v}_{ly}}{\partial t \partial y_l} ,
\end{aligned}
\tag{8}
$$

where $\tilde{b}(y_l)$ and $\tilde{\rho}_l(y_l)$ are free functions of y_l that vanish at $y_l \to -\infty$, and $\tilde{u}_l(t)$ is an arbitrary function of t. The functions $\tilde{c}(y_l)$ and $f(t)$ satisfy the following differential equations:

$$
\begin{aligned}
&\left[\frac{d^2}{dy_l^2} - k^2\right]\tilde{c} + k^2\frac{\tilde{\rho}_l}{\rho_l} = 0 \\
&\frac{df}{dt} = G(t) ,
\end{aligned}
\tag{9}
$$

where

$$
G(t) \equiv g(t) - \frac{\partial U_l}{\partial t} . \tag{10}
$$

The next step is to recognize that, using Eqs. (7) in Eq. (5c), the interface equation can be rewritten in the following form: $(\partial_t - kU_h)\tilde{\eta} = \tilde{v}_{hy}(y = 0, t)$.

After substituting Eqs. (7) and (8) into the jump conditions [Eqs. (6)] and using the differential form of the interface equation, the following ordinary differential equation for $\tilde{\eta}(t)$ is derived:

$$
\begin{aligned}
&(\partial_t - kU_l)G^{-1}\Big\{(\partial_t - kU_l)(\partial_t - kU_h)\tilde{\eta} \\
&+ A\big[kU_l(\partial_t - kU_h) + kg\big]\tilde{\eta}\Big\} \\
&- Ak^2U_h\tilde{\eta} = 0 ,
\end{aligned}
\tag{11}
$$

where

$$
A \equiv (\rho_h - \rho_l)/(\rho_h + \rho_l)
$$

is the Atwood number. For ICF applications, the appropriate ordering

$$
U_h/U_l = \rho_l/\rho_h \sim (1 - A) << 1 \text{ and } g > \partial U_l/\partial t .
$$

To lowest order in 1-A, the last term in Eq. (11) can be neglected, yielding

$$
\Big\{(\partial_t - kU_l)(\partial_t - kU_h) + A\big[kU_l(\partial_t - kU_h) + kg\big]\Big\}\tilde{\eta} = 0. \tag{12}
$$

Equation (12) can be further simplified by using the Ansatz

$$\tilde{\eta}(t) = \xi(t)\exp\left[\frac{3}{2}k\int_0^t U_h(t')dt'\right] \qquad (13)$$

and by neglecting other terms of order $(1-A) << 1$. After some straightforward manipulations, we obtain

$$\frac{d^2\xi}{dt^2} + k\left[Ag - \frac{1}{2}\frac{dV_a}{dt} - \frac{1}{4}kV_a^2\right]\xi = 0\ , \qquad (14)$$

where g and V_a are functions of time with V_a the ablation velocity. Observe that, for steady equilibrium configurations, Eqs. (13) and (14) yield the normal mode solution for $\tilde{\eta} \sim \exp(\gamma t)$, with γ satisfying the dispersion relation

$$\gamma = \sqrt{(|kg|A) + \frac{1}{4}k^2V_a^2} - \frac{3}{2}|kV_a|\ . \qquad (15)$$

It is easy to recognize that the contribution of the second term under the square root is relevant only at very small wavelengths, where the mode is already strongly stabilized by convection [the last term in Eq. (15)]. Neglecting such a term in Eqs. (14) and (15) would cause only a small shift of the cutoff wave number $[\Delta k_c/k_c = 1/9]$, which is consistent with the order of magnitude of the previous approximations. After neglecting such a term, Eq. (15) reproduces the numerically derived growth rate of Ref. 3 with β = 1.5. Equations (13) and (14), which are valid for arbitrary unsteady configurations, can now be applied to the particular equilibrium obtained by temporally modulating the laser intensity. Consider a planar target of thickness d and density ρ_0 irradiated by a uniform laser beam. The periodically modulated laser intensity $[I(t) = I_0(1+\Delta\sin\omega_0 t), \Delta \le 1]$ induces an oscillating ablation pressure $P_a(t) = P_0(1+\Delta_p\sin\omega_0 t)$ and ablation velocity $V_a(t) = V_{a0}(1+\Delta_a\sin\omega_0 t)$ with $\Delta_p \lesssim \Delta$ and $\Delta_a \lesssim \Delta$. For simplicity, we assume that the ablation pressure and the ablation velocity are directly proportional to the laser intensity, and the ablation process develops on a very slow time scale compared to an oscillation period and the sound transit time through the target [$V_a << c_s, c_s$ is the sound speed]. Although the scaling $V_a \sim \sqrt{I} \sim [1+\Delta\sin(\omega_0 t)]^{1/2}$ is more appropriate than a simple linear dependence, the numerical simulations show that the ablation velocity is almost insensitive to the oscillations in the laser intensity $(\Delta_a << 1)$ and $V_a \simeq V_{a0}$. I_0 and P_0 are two slowly varying functions of time

$$[V_a/d < (1/I_0)(dI_0/dt) = (1/P_0)(dP_0/dt) << \omega_0 \sim c_s/d].$$

A simple estimate of the acceleration of the ablation front can be derived by solving the one-dimensional compressible fluid equations of Ref. 6 for a target accelerated by the ablation pressure. As shown in Appendix B, the time-dependent acceleration can be written in the following form:

$$g(t) = -\frac{dV_a}{dt} - L^{-1}\left\{\coth\left[\frac{s}{c_s}(d-\bar{y}_a)\right]\frac{s\hat{p}_a(s)}{\rho_0 c_s}\right\}, \qquad (16)$$

where L^{-1} denotes the inverse Laplace transform, s is the Laplace variable, and $\hat{p}_a(s)$ is the Laplace transform of the ablation pressure. The quantity $\bar{y}_a = \int_0^t V_a(t')dt'$ is the position of the ablation front in the Lagrangian frame of the moving target. In deriving Eq. (16), the slow ablation time scale $(\sim d/V_a)$ has been treated as an independent variable. A simple expression for $g(t)$ can be derived in the asymptotic limit $(d/V_a) > t >> (d/c_s)$, yielding

$$g(t) = -g_0[1+\alpha\sin\omega_0 t + \epsilon\cos\omega_0 t]\ , \qquad (17)$$

where $g_0 \equiv P_0/\rho_0 d_a$, $\alpha \equiv \Delta_p(\omega_0 d_a/c_s)\cot(\omega_0 d_a/c_s)$, and $\epsilon = V_{a0}\,\Delta_a\omega_0/g_0$, $d_a = d - \bar{y}_a$. A more accurate estimate of $g(t)$ (and of the parameters g_0, α, and ϵ) can be obtained by using a one-dimensional code. Later in this article we will use the one-dimensional hydrodynamic code *LILAC*[7] to derive g_0, α, and ϵ. However, Eq. (17) gives some physical insight into the relevant quantities that affect the oscillation amplitude in the target acceleration. In particular, large oscillations can be achieved for values of the modulation period shorter than the sound transit time through the target $[T_0 \equiv 2\pi/\omega_0 < d/c_s]$. Before proceeding further, it is important to define the range of validity of the stability model for the prescribed equilibrium. The oscillations in the ablation pressure propagate inside the target at the sound speed. Thus, the equilibrium parameters can be considered as uniform over a distance $\Delta y < c_s T_0$. The stability analysis, carried out for a uniform semi-infinite medium, can be applied to perturbations with sufficiently short wavelength $k\Delta y > 1$. It follows that a necessary condition for the validity of the stability model is $kc_s T_0 >> 1$. For such wavelengths, Eq. (17) can be used in

Eq. (14) to derive the function $\xi(t)$. Thus, Eq. (14) can be written in the following form:

$$\frac{d^2\xi}{dt^2} - \gamma_c^2\left[1 + q\sin(\omega_0 t + \phi)\right]\xi = 0 \ , \tag{18}$$

where $\gamma_c = \sqrt{A|kg_0|}$ is the classical growth rate,

$$q = \sqrt{\alpha^2 + 9\epsilon^2/4} \ ,$$

and

$$\phi = \tan^{-1}(3\epsilon/2\alpha) .$$

Notice that Eq. (18) is a Mathieu equation, whose solution has the form $\xi(t) = \sigma(t)\exp(\mu t)$, with $\sigma(t)$ being periodic with period ω_0. Using Eq. (13), the growth rate of the instability can be easily derived:

$$\gamma = -k\beta\frac{1}{T_0}\int_0^{T_0} V_a(t')dt' + \mu , \tag{19}$$

where β = 1.5 for the simplified stability model. However, when Eq. (19) is compared to the Takabe formula, we let $\beta = \beta^T = 3-4$. In order to find μ, one needs to numerically solve Eq. (18) for one period of oscillation. Figure 57.2 shows the parameter μ, plotted versus the wave number k, for the following equilibrium parameters: d = 20 μm, $g_0 = 5 \times 10^{15}$ cm/s^2, A = 1, $\langle V_a \rangle = 7 \times 10^4$ cm/s, $c_s = 10^6$ cm/s, $T_0 = 0.3 \times 10^{-9}$ s, ϕ = 0, and q = 0, 2.5, and 3.5. The validity of the stability model requires $\lambda = 2\pi/k << 20\,\mu$m. For any value of q and ω_0, it is possible to identify intervals of the k axis, where $Re[\mu]$ = 0. We denote such intervals as dynamically stabilized (DS) regions, and we emphasize the importance of ablative convection [see Eq. (19)] at shorter wavelengths. According to Eqs. (1) and (19), the short-wavelength modes are stabilized by convection, and the cutoff wave number is $k_c = gA/\beta^2 V_A^2$. It follows that an efficient dynamic stabilization can be achieved by choosing values of q and ω_0 that cause the first DS region to be located inside the interval $0 < k < k_c$. In Fig. 57.3, the growth rates derived from Eq. (19) for q = 0, 2.5, and 3.5 and β = 3.5 (as given by Takabe *et al.*[3]) are shown. Observe that as q increases, a better stabilization is induced at longer wavelengths, but shorter wavelengths can be destabilized (q = 3.5). This short-wavelength instability is driven by the oscillations in the acceleration, with the perturbation having the characteristic structure of an oscillatory mode with an exponentially increasing amplitude. For convenience, we denote these short-wavelength modes as "parametric instabilities."

Furthermore, when the mode wavelength is smaller than the density gradient scale length

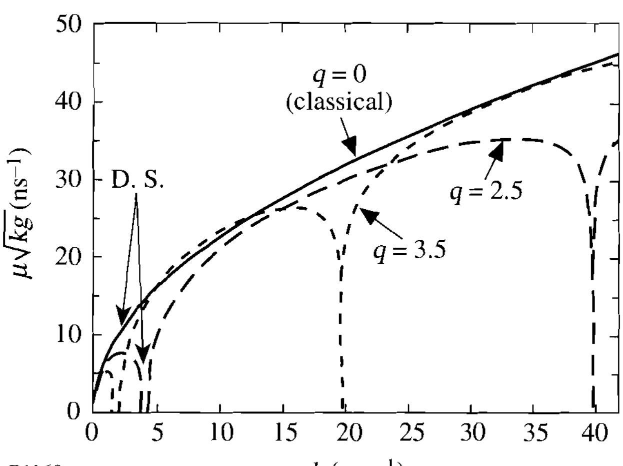

Figure 57.2
Plot of the instability drive term μ versus the mode wave number k for modulated ($q \neq 0$) and unmodulated ($q = 0$) laser intensity, assuming d = 20 μm, $g_0 = 5 \times 10^{15}$ cm/s^2, the Atwood number A = 1, $\langle V_a \rangle = 7 \times 10^4$ cm/s, T_0 = 0.3 ns, and ϕ = 0.

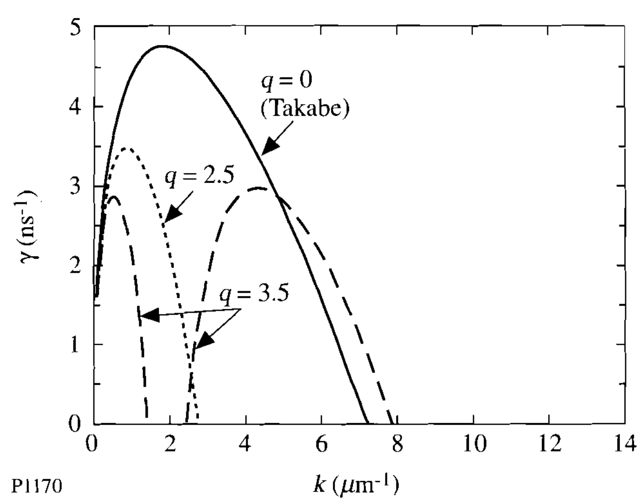

Figure 57.3
Plot of the instability growth rate versus the mode wave number k for modulated ($q \neq 0$) and unmodulated ($q = 0$) laser intensity, assuming the same equilibrium parameters as in Fig. 57.1.

$$\left[\delta = \left|(1/\rho)\,d\rho/dy\right|^{-1}\right],$$

the sharp boundary model is not valid and Eq. (19) cannot be used.

The results of the analytic theory have been compared with two-dimensional simulations obtained using the code *ORCHID*.[8] We have considered an 18-μm CH planar target irradiated by a uniform laser beam of wavelength 1.06 μm. The laser intensity is modulated in time with a period of 0.3 ns. The modulation amplitude is 100%, and the flat-top average intensity is 50 TW/cm^2. For an accurate comparison with the analytic stability theory, we derive the equilibrium parameters g, $\langle V_a \rangle$, and q from the one-dimensional code *LILAC*.[7] The result is $g = 4.5 \cdot 10^{15}\,\mathrm{cm/s^2}$, $\langle V_a \rangle = 7 \cdot 10^4\,\mathrm{cm/s}$, $\delta \simeq 1.5$ to 2 μm, $\phi = 0$, and $q = 3.5$ to 5.5. In the two-dimensional simulation, an initial single-wavelength perturbation evolves for 3 ns. Because of the short modulation period, the simulation shows no significant change in the foil isentrope with respect to the unmodulated case. Figure 57.4 shows a comparison between the linear growth rate derived from the simulation with the one given by Eq. (19). Three regions of the k-axis can be identified: (1) The long-wavelength region with $k < 0.2\ \mu\mathrm{m}^{-1}$, where the growth rate is virtually insensitive to the modulation of the laser intensity and very close to the classical value. (2) The intermediate wavelength region with $0.2 < k < 1$. For these values of the wave number, the dynamic stabilization is particularly effective. Observe that for $\lambda = 2\pi/k \approx 7\,\mu$m the mode is completely stabilized. (3) The short-wavelength region is defined as having a wave number $k > 1$. In this region $k\delta > 1$ and the effect of finite density-gradient scale length cannot be neglected. Notice that the simulation shows the presence of an unstable mode with wavelength $\lambda \approx 5\ \mu$m. Using Eq. (19) beyond its limit of validity ($k\delta < 1$) and dividing γ_c^2 by $(1 + \theta k\delta)$ with $\theta < 1$, we would predict the existence of parametric instabilities at shorter wavelengths (Fig. 57.4). However, the structure of the perturbation observed in the numerical simulation does not clearly show the characteristics of a parametric instability. Furthermore, the cutoff wave number observed in the numerical simulation (with or without laser-intensity modulation) is much shorter than the one predicted by Eqs. (1) and (19). The stability of very-short-wavelength perturbations needs further investigation to determine an accurate value of the cutoff wave number.

The dynamic stabilization of the Rayleigh-Taylor instability in ICF targets was first observed in numerical simulations by J. Boris.[9] In this article we have shown the derivation of the linear stability theory for unsteady ablation fronts and the conditions for the dynamic stabilization of the ablative Rayleigh-Taylor instability. The growth rate of the instability has been calculated for a sinusoidal modulation of the laser intensity. It is shown that an appropriate modulation frequency and amplitude can stabilize a large portion of the unstable spectrum and significantly reduce the maximum growth rate.

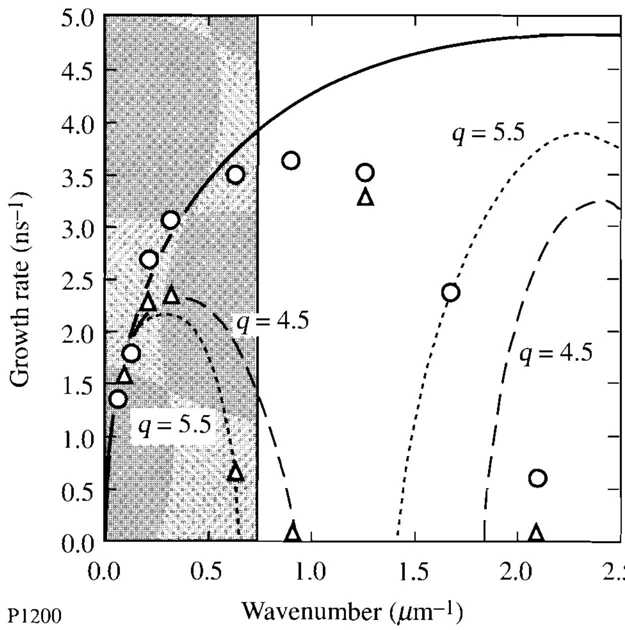

Figure 57.4
Comparison of the growth rate obtained from numerical simulations (with modulation Δ and without modulation O) and the modified Eq. (19). Here, $d = 18\ \mu$m, $g_0 = 4.5 \times 10^{15}$ cm/s^2, $\langle V_a \rangle = 7 \times 10^4$ cm/s, $T_0 = 0.3$ ns, $\phi = 0$, $A = 1$, $\beta = 3$, $\theta\delta = 1.5 \times 10^{-5}$ cm, $q = 5.5$ (dotted), $\beta = 4$, $\theta\delta = 0.3 \times 10^{-5}$ cm, $q = 4.5$ (dashed). The solid line represents the Takabe formula, and the shaded area represents the region with $\kappa\delta \lesssim 1$.

ACKNOWLEDGMENT

This work was supported by the U.S. Department of Energy Office of Inertial Confinement Fusion under Cooperative Agreement No. DE-FC03-92SF19460, the University of Rochester, and the New York State Energy Research and Development Authority. The support of DOE does not constitute an endorsement by DOE of the views expressed in this article.

APPENDIX A: CONDITIONS FOR INCOMPRESSIBLE FLOW

A better model for the Rayleigh-Taylor instability can be obtained by replacing the incompressibility condition with an adiabatic equation of state. In the heavy- and light-fluid regions, where the velocity and density equilibrium profiles are uniform, the linearized adiabatic equation of state can be written as

$$\left(\partial_t + U_j\partial_y\right)\tilde{p}_j + \tilde{v}_{jy}\frac{dP_J}{dy} + \frac{5}{3}P_j\nabla\cdot\tilde{v}_j = 0, \quad \text{(A.1)}$$

where P_j represents the equilibrium pressure in the region j. Ordering $\partial_t \sim \sqrt{kg} \sim kU_h$ and using the momentum conservation equation, one finds that $\tilde{p}_j \sim \rho_j U_j \tilde{v}_j$, $\partial_y \tilde{p}_j \sim k\tilde{p}_j$, and $\left(dP_J/dy\right) \sim \rho g$. A simple comparison between the two terms in Eq. (A.1) yields

$$\frac{P_j\nabla\cdot\tilde{v}_j}{\left(\partial_t + U_j\partial_y\right)\tilde{p}_j + v_{jy}\left(dP_J/dy\right)} \sim \frac{1}{M_j^2}, \quad \text{(A.2)}$$

where $M_j^2 = 3\rho_j U_j^2/5P_j$ is the Mach number in region j. For subsonic flows ($M_j << 1$), Eq. (A.1) leads to the incompressibility condition $\nabla\cdot\tilde{v}_j \simeq 0$. Although the flow in the two regions is clearly incompressible, at the interface between the fluids, where the equilibrium velocity and density have very sharp gradients, the conclusions derived above do not immediately apply.

A jump condition relating the energies in the two regions can be derived by integrating the adiabatic equation of state across the ablative layer. Following the work of Ref. 2, the calculation can be greatly simplified by using the conservative form of the equation of state:

$$\partial_t\left(\frac{1}{2}\rho v^2 + \frac{3}{2}p\right) + \nabla\cdot\left[\left(\frac{1}{2}\rho v^2 + \frac{5}{2}p\right)\mathbf{v}\right]$$

$$= \rho\mathbf{g}\cdot\mathbf{v} + I\delta\left(y - \tilde{\eta}\right), \quad \text{(A.3)}$$

where I is the power deposited at the ablation front. Integrating Eq. (A.3) and linearizing the variables yields the following jump condition for the fluid energy:

$$\partial_t\tilde{\eta}\left(\rho_h U_h^2 - \rho_l U_l^2\right) + \left(\frac{3}{2}\rho_h U_h^2 + \frac{5}{2}P_h\right)\tilde{v}_{hy}$$

$$-\left(\frac{3}{2}\rho_l U_l^2 + \frac{5}{2}P_l\right)\tilde{v}_{ly} + \frac{5}{2}\tilde{p}_h U_h$$

$$-\frac{5}{2}\tilde{p}_l U_l - \frac{1}{2}\tilde{\rho}_l U_l^3 = 0, \quad \text{(A.4)}$$

where all the quantities are calculated at the unperturbed ablation front ($y = 0$). In the derivation of Eq. (A.4), the incompressible results in the two regions have been used. The ordering for the perturbed quantities can be derived from the conservation equations

$$\partial_t\tilde{\eta} \sim \tilde{v}_{hy}/kU_h \qquad \tilde{p}_j \sim \rho_j U_j \tilde{v}_j \qquad \tilde{\rho}_l \sim \rho_h\tilde{v}_{hy}/U_l \quad \text{(A.5)}$$

Substituting the relations in Eq. (A.5) into Eq. (A.4) yields the following equation for the perturbed normal velocities at the ablation front:

$$\left[1 + O\left(M_h^2\right)\right]\tilde{v}_{hy} = \left[1 + O\left(M_l^2\right)\right]\tilde{v}_{ly} \quad \text{(A.6)}$$

For $M_j^2 \to 0$, Eq. (A.6) reduces to

$$\tilde{v}_{hy} = \tilde{v}_{ly}. \quad \text{(A.7)}$$

Observe that the latter can also be derived from the incompressibility condition $\left(\nabla\cdot\mathbf{v} = 0\right)$ integrated across the ablative layer. Thus, the assumption of incompressible flow holds at the ablation front as well as at the two uniform regions on both sides of the interface when the Mach number is much less than unity, i.e., the flow is subsonic.

APPENDIX B: UNSTEADY EQUILIBRIUM OF AN ACCELERATED TARGET

The time evolution of the equilibrium of a planar target accelerated by an externally applied pressure $P_a(t)$ can be obtained by solving the one-dimensional fluid equations of Ref. 6. In ICF the accelerating pressure is induced by the laser irradiation. In order to simplify the calculation, we rewrite the fluid equations in a Lagrangian frame, and we neglect the reduction of the target thickness due to ablation. Let $y_T(\bar{y},t)$ be the trajectories of the fluid elements and $\bar{y}$ the Lagrangian coordinate: i.e., the position of the fluid elements at time $t = 0$. As shown in Ref. 6, a linear wave equation describing the evolution of the fluid trajectories can be derived from the nonlinear set of equations

$$\frac{\partial^2 y_T}{\partial t^2} = c_s^2 \frac{\partial^2 y_T}{\partial \bar{y}^2}, \tag{B.1}$$

where c_s is the sound speed of the target at rest. We consider a planar target of thickness $d(0 \le \bar{y} \le d)$ with the irradiated side at $\bar{y} = 0$ $[p(0,t) = P_a(t)]$. On the surface opposite to the laser $(\bar{y} = d)$, the external pressure is negligible $[p(d,t) = 0]$. These boundary conditions lead to the following equations for the trajectories at $\bar{y} = 0$ and $\bar{y} = d$:

$$\frac{\partial y_T}{\partial \bar{y}}(0,t) = 1 - \frac{P_a(t)}{\rho c_s^2} \qquad \frac{\partial y_T}{\partial \bar{y}}(d,t) = 1\,. \tag{B.2}$$

We let the laser irradiation start at time $t = 0$ (target at rest). Thus, the velocity at $t = 0$ is zero through the target:

$$\frac{\partial y_T}{\partial t}(\bar{y},0) = 0 \qquad y_T(\bar{y},0) = \bar{y}\,. \tag{B.3}$$

Equation (B.1), together with the boundary and initial conditions [Eqs. (B.2) and (B.3)], can be solved in the Laplace transform domain. A short calculation yields the following form of the Laplace transform (L) of the acceleration:

$$\hat{g}(s,\bar{y}) = \frac{\hat{P}(s)}{\rho c_s}\, s \,\frac{\cosh\left[\dfrac{s}{c_s}(d-\bar{y})\right]}{\sinh\left(\dfrac{sd}{c_s}\right)}, \tag{B.4}$$

where

$$g(\bar{y},t) = \frac{\partial^2 y_T}{\partial t^2} \qquad \hat{g}(\bar{y},s) = L[g(\bar{y},t)]$$
$$\hat{P}_a(s) = L[P_a(t)] \tag{B.5}$$

and s is the Laplace variable. Using the identity

$$\frac{1}{\sinh z} \equiv 2\sum_{n=0}^{\infty} e^{-(2n+1)z}$$

and taking the inverse transform of Eq. (B.4), we obtain the acceleration of the ablation front

$$g(0,t) = \frac{1}{\rho c_s}\left\{\frac{dP_a}{dt}\left[t - \frac{\bar{y}}{c_s}\right] + 2\sum_{n=1}^{\infty}\frac{dP_a}{dt}\left[t - \frac{2nd}{c_s}\right]\Theta\left[t - \frac{2nd}{c_s}\right]\right\}, \tag{B.6}$$

where $\Theta(t)$ is the Heaviside step function. Focusing on an oscillating applied pressure induced by an oscillating laser intensity

$$\left[P_a(t) = P_0\left(1 + \Delta_p \sin\omega_0 t\right)\right],$$

we determine the asymptotic value of the acceleration after many periods of the oscillation $(t\omega_0 >> 1)$. A short calculation yields

$$g(0,t) = \frac{P_0}{\rho d}\left(1 + \alpha \sin\omega_0 t\right), \tag{B.7}$$

where $\alpha = \Delta_p(\omega_0 d/c_s)\cot(\omega_0 d/c_s)$. The first term on the RHS represents the incompressible component of the acceleration. The other terms are induced by the oscillation in the applied pressure and vanish for $c_s \to \infty$, i.e., incompressible fluid. Observe that Eq. (B.7) yields the resonant condition for the oscillations, $\omega_0 d/\pi c_s = n$, where $n = 1,2,\ldots$.

A more accurate expression of the acceleration can be obtained by retaining the effect of finite ablation velocity (V_a). For a subsonic ablation flow ($V_a << c_s$) and times shorter than the ablation time $\left(2\pi/\omega_0 << t << d/V_a\right)$, the ablative flow can be treated as a perturbation of the equilibrium. Thus, the acceleration becomes

$$g(0,t) = g_0\left(1 + \alpha \sin \omega_0 t + \in \cos \omega_0 t\right), \qquad \text{(B.8)}$$

where $g_0 = P_0/\rho d_a$, $d_a = d - \int_0^t V_a dt'$ is the target thickness at time t, and the ablation velocity has been taken proportional to the laser intensity $\left[V_a = V_{a0}\left(1 + \Delta_a \sin \omega_o t\right) \propto I(t)\right]$. For typical ICF parameters and oscillation periods of the order of hundreds of picoseconds, the term $\in = \Delta_a V_{a0} \omega_0 / g_0$ is much less than unity and can be neglected.

REFERENCES

1. Lord Rayleigh, *Scientific Papers* (Cambridge University Press, Cambridge, England, 1900), Vol. II, p. 200.
2. S. E. Bodner, Phys. Rev. Lett. **33**, 761 (1974).
3. H. Takabe, K. Mima, L. Montierth, and R. L. Morse, Phys. Fluids **28**, 3676 (1985).
4. H. J. Kull and S. I. Anisimov, Phys. Fluids **29**, 2067 (1986).
5. A. B. Bud'ko and M. A. Liberman, Phys. Rev. Lett. **68**, 178 (1992).
6. N. Rostoker and H. Tahsiri, Comments Plasma Phys. Cont. Fusion **3**, 39 (1977).
7. E. B. Goldman, Laboratory for Laser Energetics Report No. 16, 1973 (unpublished); J. Delettrez and E. B. Goldman, Laboratory for Laser Energetics Report No. 36, 1976 (unpublished).
8. R. L. McCrory and C. P. Verdon, *Computer Applications in Plasma Science and Engineering*, edited by Adam T. Drobot (Springer-Verlag, NY, 1991), pp. 291–325.
9. J. P. Boris, Comments Plasma Phys. Cont. Fusion **3**, 1 (1977).